SUPPORTING INFORMATION
For
Rapid Prediction of Adsorption Isotherms of a Diverse Range of Molecules in Hyper-Crosslinked Polymers

Dai Tang[1], Grit Kupgan[2], Coray M. Colina[2,3], David S. Sholl[1,*]
[1] School of Chemical & Biomolecular Engineering, Georgia Institute of Technology, Atlanta, GA 30332-0100, USA
[2] Department of Materials Science and Engineering, University of Florida, Gainesville, FL 32611-7200, USA
[3] Department of Chemistry, University of Florida, Gainesville, FL 32611-7200, USA
Corresponding author: E-mail: david.sholl@chbe.gatech.edu

Table of contents

1) Structural properties of HCPs as functions of percentage of DVB and degree of crosslinking
2) Physical properties of molecules and force field parameters for HCPs
3) Calculated helium void fraction of HCPs and heat of adsorption for each molecule-HCP pair
4) Scaling factors
5) Estimated selectivity of molecular pairs using Freeman's model
6) Examples: check the convergence of GCMC simulations
7) Data shown in all figures in the main manuscript in tabular form
8) Supporting information references

1) Structural properties of HCPs as functions of percentage of DVB and degree of crosslinking

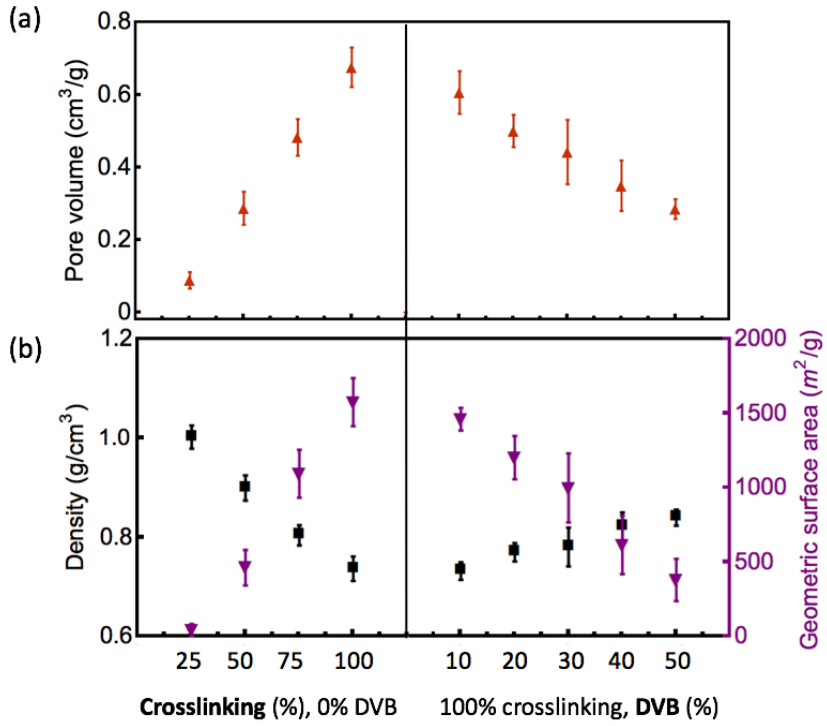

Figure S1: The effect of crosslinking and DVB on pore volume, density and geometric surface area of HCPs. The left panels show data as function of degree of crosslinking, and the right panels show data as function of percentage of DVB.

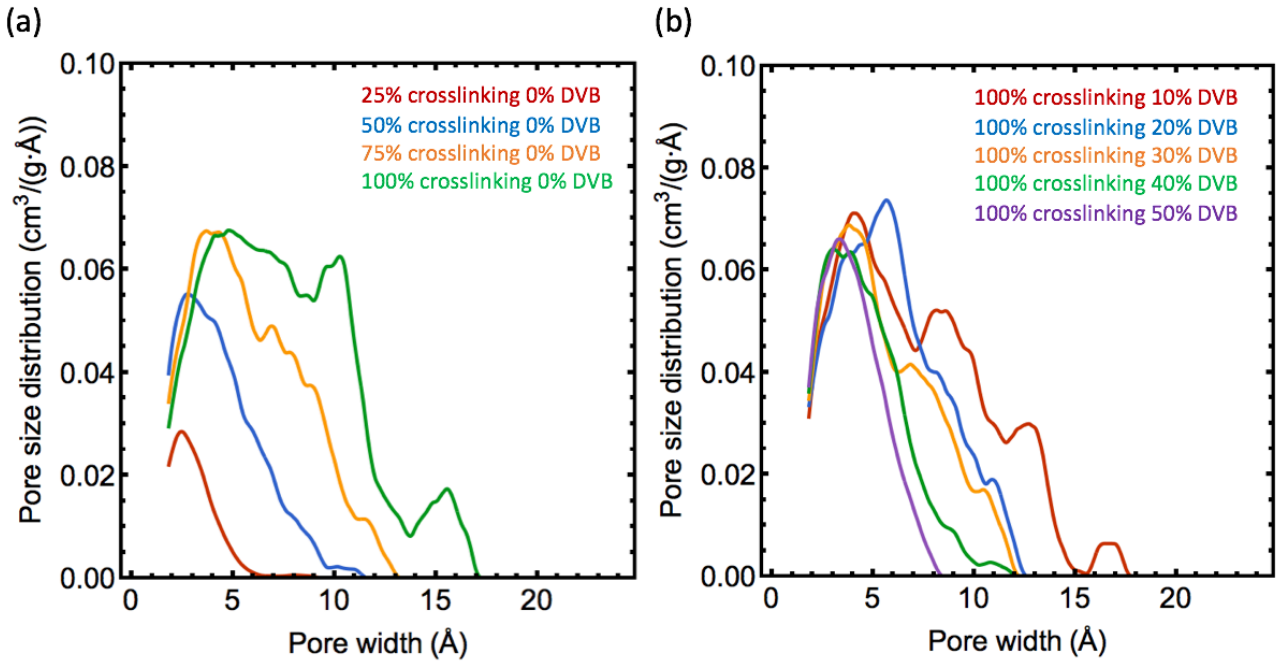

Figure S2: The effect of crosslinking and DVB on pore size distribution. The plots show the averaged results among 5 samples of each HCP.

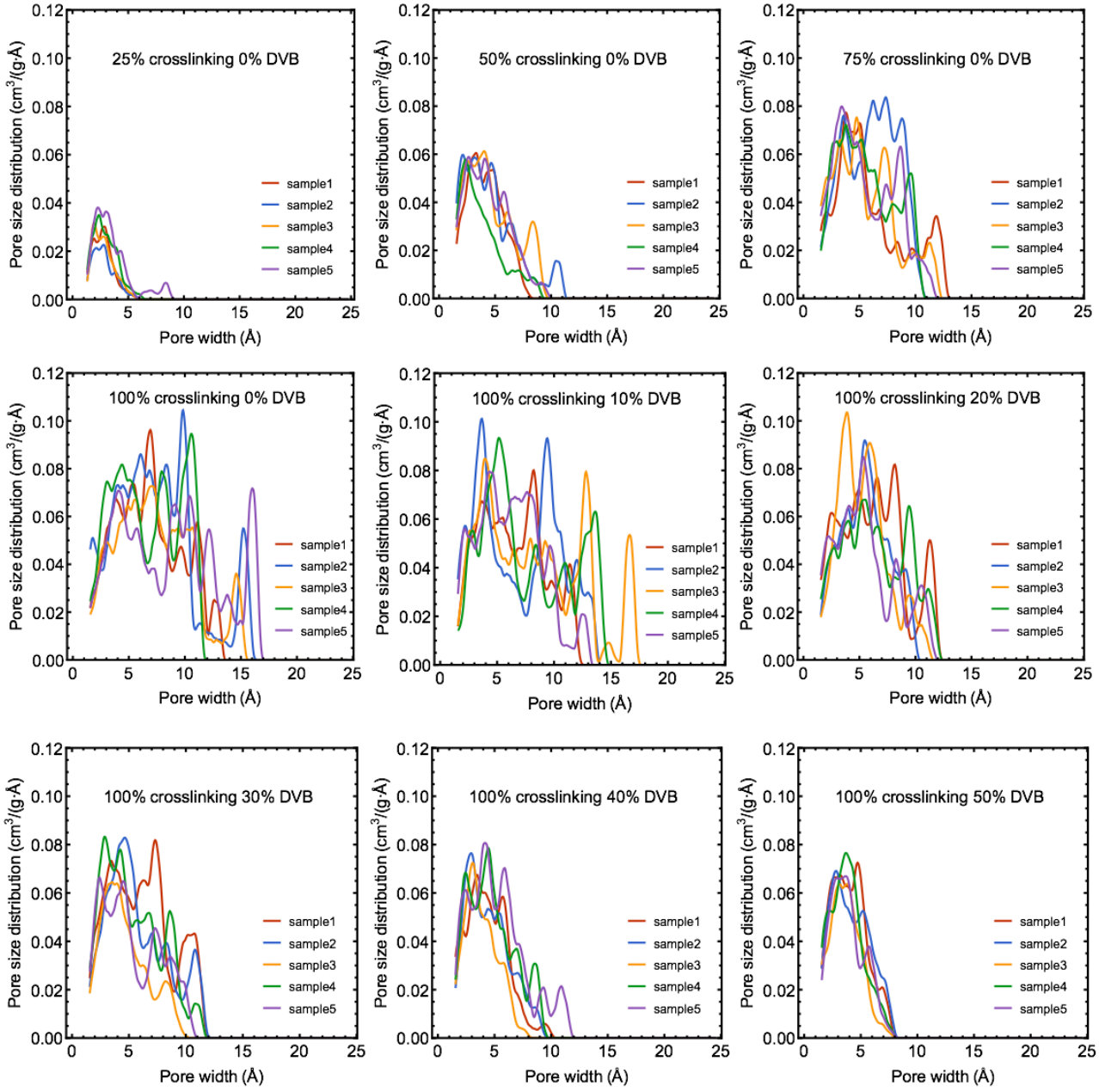

Figure S3: Pore size distribution in 5 samples of each HCP with different degrees of crosslinking and percentages of DVB.

2) Physical properties of molecules and force field parameters for HCPs

Table S1. List of molecular weight, bulk liquid density, critical temperature and vapor pressure of 24 molecules in this study.[1-8]

Chemical formula	Name	Molecular weight (g/mol)	Bulk liquid density (g/cm^3)	Critical temperature (K)	Vapor pressure (Pa)
CH_4	Methane	16.04	0.16	190.6	4520000
C_2H_4	Ethene	28.05	0.22	282.4	3550430
C_2H_6	Ethane	30.07	0.30	305.3	3845280
C_2H_3N	Acetonitrile	41.05	0.78	549.0	11153
C_3H_6	Propene	42.08	0.50	365.6	1560410
C_2H_4O	Acetaldehyde	44.05	0.78	463.4	116078
C_3H_8	Propane	44.10	0.49	369.8	1023210
C_2H_6O	Dimethyl ether	46.07	0.65	398.0	623460
CH_4S	Methanethiol	48.11	0.86	475.0	210719
C_3H_5N	Propionitrile	55.08	0.77	556.0	6287
C_3H_6O	Acetone	58.08	0.70	508.0	31925
C_3H_8O	Propan-1-ol	60.10	0.80	538.0	3878
C_3H_8O	Propan-2-ol	60.10	0.79	502.0	11634
C_2H_6S	Dimethyl sulfide	62.13	0.85	504.0	69029
C_2H_6S	Ethanethiol	62.13	0.86	502.0	76657
Kr	Krypton	83.80	0.91	209.5	5100000
C_4H_4S	Thiophene	84.14	1.05	605.0	12359
$C_5H_{10}O$	2-pentanone	86.13	0.81	561.0	5180
$C_4H_{10}S$	Diethyl sulfide	90.19	0.83	562.0	8680
C_7H_8	Toluene	92.14	0.87	593.0	4182
$C_6H_{14}O$	Dipropyl ether	102.17	0.75	527.0	8972
$C_8H_{16}O$	Octanal	128.21	0.82	627.2	201.8
$C_8H_{18}O$	Octan-1-ol	130.23	0.82	629.0	46.64
Xe	Xenon	131.29	1.10	289.7	3183600

Table S2. Lennard-Jones parameters for united atoms of HCPs.[2, 9]

United atoms	ε/k_B **(K)**	σ **(Å)**
Lc1	10.0	4.65
Lc2	46.0	3.95
Cc0	21.0	3.88
Ccp	50.50	3.695
c1	10.0	4.65
c2	46.0	3.95

In this study, no charges are used for the united atoms of HCPs. In order to test this approximation, we constructed all-atom models of each monomer and optimized each monomer at the PBE-D3 level of DFT using VASP. From the resulting electron densities, we assigned DDEC6 charges to the atoms of each monomer. The atomic charges in these HCP all-atom models are relatively small and can be neglected for the UAFF selected in this work (Figure S4 and Table 3).

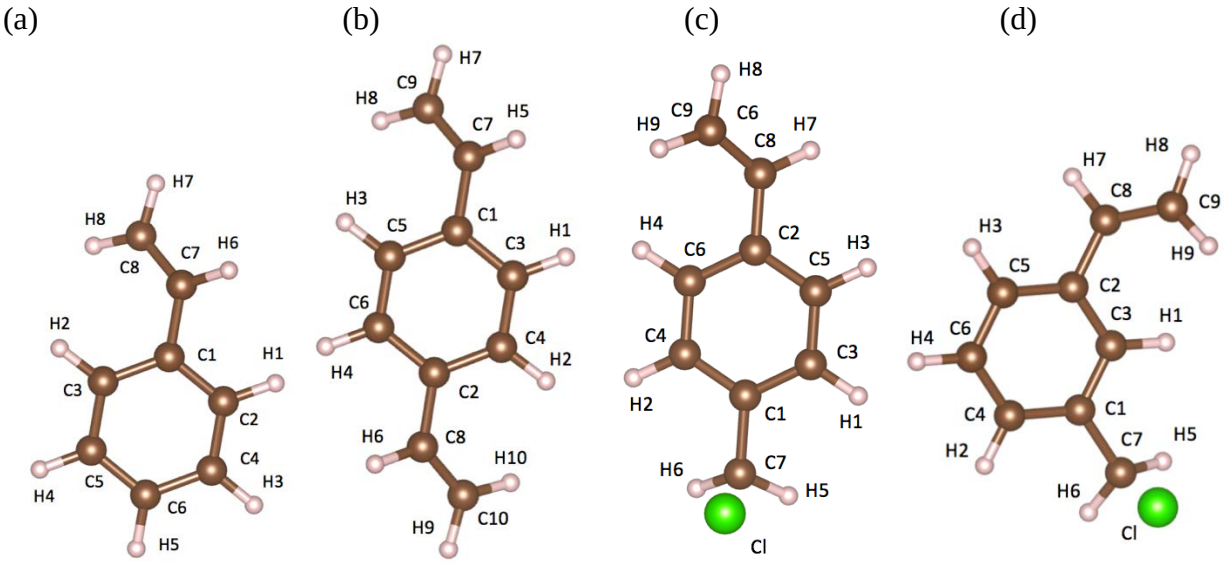

Figure S4: Structure of all atom models of (a) styrene (b) divinylbenzene (c) p-vinylbenzyl chloride and (d) m-vinylbenzyl chloride

Table 3. DDEC6 charges of atoms of all atom model of monomers. (a) styrene (b) divinylbenzene (c) p-vinylbenzyl chloride and (d) m-vinylbenzyl chloride.

(a) net charge= 10^{-6} e

Atom	Charge	United atom
C1	0.104712	Cc0
C2	-0.138522	Ccp
C3	-0.122986	Ccp
C4	-0.087447	Ccp
C5	-0.088714	Ccp
C6	-0.093552	Ccp
C7	-0.070253	Lc1
C8	-0.323909	Lc2
H1	0.095436	Ccp
H2	0.098029	Ccp
H3	0.09564	Ccp
H4	0.095724	Ccp
H5	0.088209	Ccp
H6	0.090308	Lc1
H7	0.127517	Lc2
H8	0.129807	Lc2

United Atom	Charge
Lc1: C7, H6	0.020055
Lc2: C8, H7, H8	-0.066585
Cc0: C1	0.104712
Ccp: C2, H1	-0.043086
Ccp: C3, H2	-0.024957
Ccp: C4, H3	0.008193
Ccp: C5, H4	0.00701
Ccp: C6, H5	-0.005343

(b) net charge=0 e

Atom	Charge	United atom

United atom	Charge

C1	0.101598	Cc0
C2	0.101675	Cc0
C3	-0.133599	Ccp
C4	-0.122374	Ccp
C5	-0.122987	Ccp
C6	-0.133753	Ccp
C7	-0.072112	Lc1
C8	-0.072838	Lc1
C9	-0.316638	Lc2
C10	-0.316224	Lc2
H1	0.095327	Ccp
H2	0.098999	Ccp
H3	0.099152	Ccp
H4	0.095385	Ccp
H5	0.089626	Lc1
H6	0.089666	Lc1
H7	0.128419	Lc2
H8	0.131147	Lc2
H9	0.128322	Lc2
H10	0.131209	Lc2

Lc1: C7, H5	0.017514
Lc1: C8, H6	0.016828
Lc2: C9, H7, H8	-0.057072
Lc2: C10, H9, H10	-0.056693
Cc0: C1	0.101598
Cc0: C2	0.101675
Ccp: C3, H1	-0.038272
Ccp: C4, H2	-0.023375
Ccp: C5, H3	-0.023835
Ccp: C6, H4	-0.038368

(c) net charge= 0 e

Atom	**Charge**	**United atom**
Cl	-0.160652	Cl
C1	0.091238	Cc0
C2	0.109142	Cc0
C3	-0.131939	Ccp
C4	-0.132645	Ccp
C5	-0.127985	Ccp
C6	-0.118303	Ccp
C7	-0.114105	Cc2
C8	-0.080115	Lc1
C9	-0.302446	Lc2
H1	0.101823	Ccp
H2	0.101904	Ccp
H3	0.100676	Ccp
H4	0.101476	Ccp
H5	0.112022	Cc2
H6	0.1123	Cc2
H7	0.087661	Lc1
H8	0.122294	Lc2
H9	0.127654	Lc2

United atom	**Charge**
Lc1: C8, H7	0.007546
Lc2: C9, H8, H9	-0.052498
Cc0: C1	0.091238
Cc0: C2	0.109142
Ccp: C3, H1	-0.030116
Ccp: C4, H2	-0.030741
Ccp: C5, H3	-0.027309
Ccp: C6, H4	-0.016827
Cc2: C7, H5, H6	0.110217
Cl	-0.160652

(d) net charge=10^{-6} e

Atom	Charge	United atom
Cl	-0.147183	Cl
C1	0.095714	Cc0
C2	0.113309	Cc0
C3	-0.171148	Ccp
C4	-0.139189	Ccp
C5	-0.13209	Ccp
C6	-0.079322	Ccp
C7	-0.11314	Cc2
C8	-0.076674	Lc1
C9	-0.310624	Lc2
H1	0.100915	Ccp
H2	0.10139	Ccp
H3	0.100685	Ccp
H4	0.096527	Ccp
H5	0.112874	Cc2
H6	0.110156	Cc2
H7	0.0843	Lc1
H8	0.123625	Lc2
H9	0.129874	Lc2

United atom	Charge
Lc1: C8, H7	0.007626
Lc2: C9, H8, H9	-0.057125
Cc0: C1	0.095714
Cc0: C2	0.113309
Ccp: C3, H1	-0.070233
Ccp: C4, H2	-0.037799
Ccp: C5, H3	-0.031405
Ccp: C6, H4	0.017205
Cc2: C7, H5, H6	0.10989
Cl	-0.147183

3) Calculated helium void fraction of HCPs and heat of adsorption for each molecule-HCP pair

Table S3. List of helium void fraction of each sample of HCPs.

HCP	Helium void fraction f_{He}				
	Sample 1	**Sample 2**	**Sample 3**	**Sample 4**	**Sample 5**
25% crosslinking 0% DVB	0.07	0.076	0.078	0.11	0.12
50% crosslinking 0% DVB	0.23	0.28	0.28	0.22	0.26
75% crosslinking 0% DVB	0.39	0.44	0.38	0.39	0.40
100% crosslinking 0% DVB	0.46	0.53	0.48	0.50	0.51
100% crosslinking 10% DVB	0.45	0.47	0.49	0.47	0.47
100% crosslinking 20% DVB	0.43	0.41	0.38	0.42	0.39
100% crosslinking 30% DVB	0.42	0.38	0.31	0.36	0.34
100% crosslinking 40% DVB	0.29	0.27	0.24	0.30	0.33
100% crosslinking 50% DVB	0.26	0.27	0.22	0.21	0.23

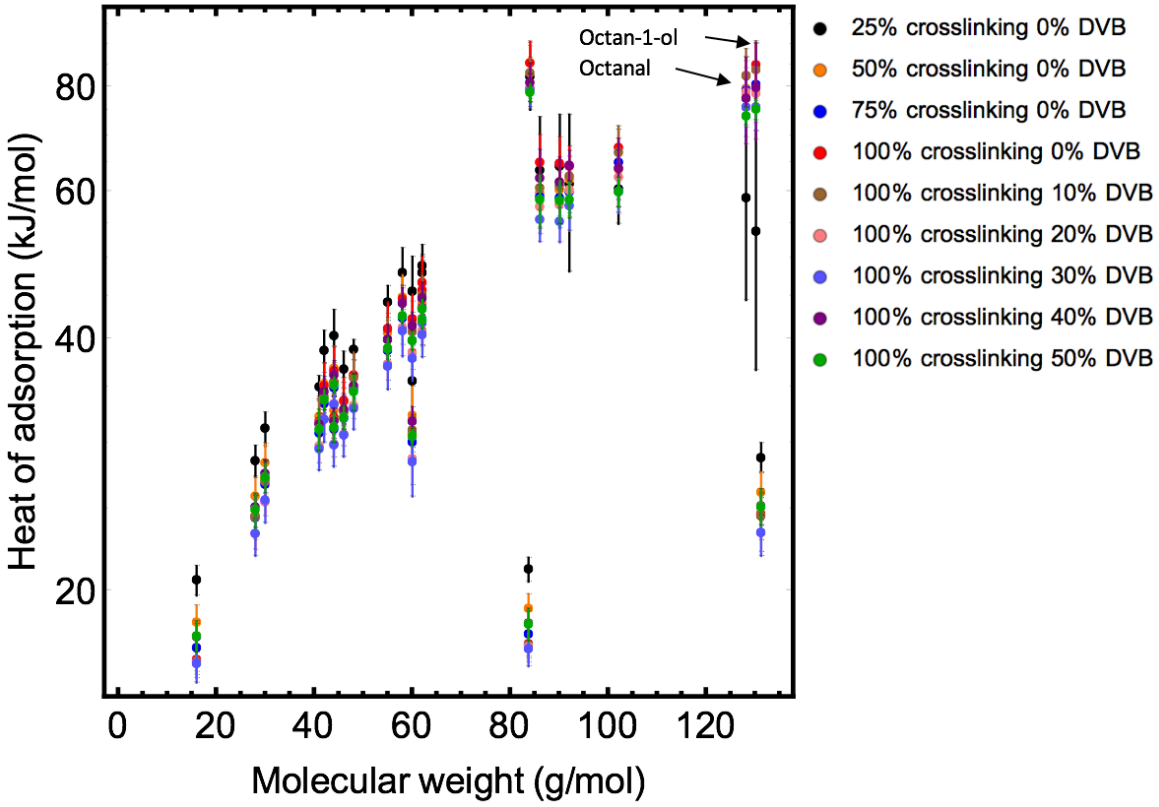

Figure S5: Heat of adsorption as function of molecular weight.

4) Scaling factors

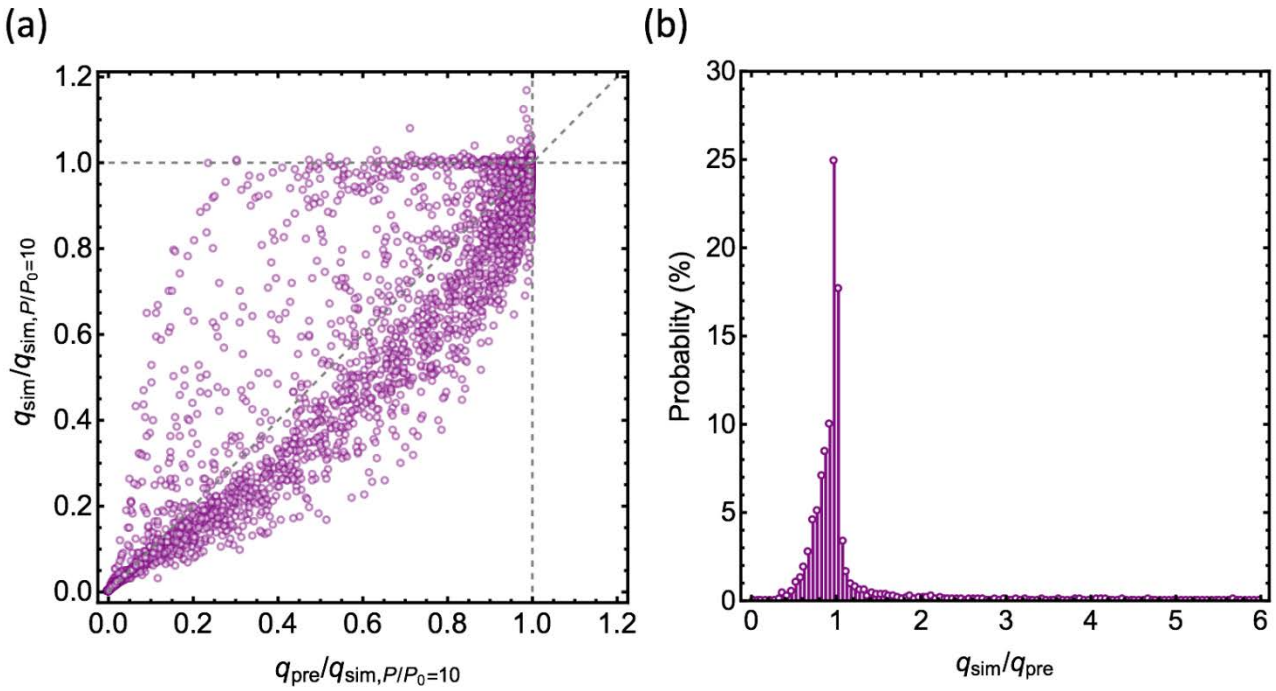

Figure S6: (a) Comparison of simulated adsorption loadings q_{sim} and predicted adsorption loadings q_{pre} for all molecule-HCP pairs, where the loadings are normalized by the simulated results at P/P_0=10 in the corresponding isotherms. The q_{pre} are estimated by using the simulated Henry's constants and simulated saturation loadings in Langmuir model (q_{sat} = $q_{sim,P/P0=10}$). All data are the averaged results among 5 samples for each HCP. About 16% of simulated adsorption loadings have $q_{sim}/q_{sim,P/P0=10}$ > 1.0, but they are equal to $q_{sim,P/P0=10}$ within the standard deviation of loadings in 5 samples. (b) Distribution of the ratio of q_{sim}/q_{pre} of adsorption loadings for all molecule-HCP pairs.

The simulated and predicted adsorption isotherms of all molecule-HCP pairs in the form of Excel spreadsheets are available in the sub-folder of the accompanying .zip file.

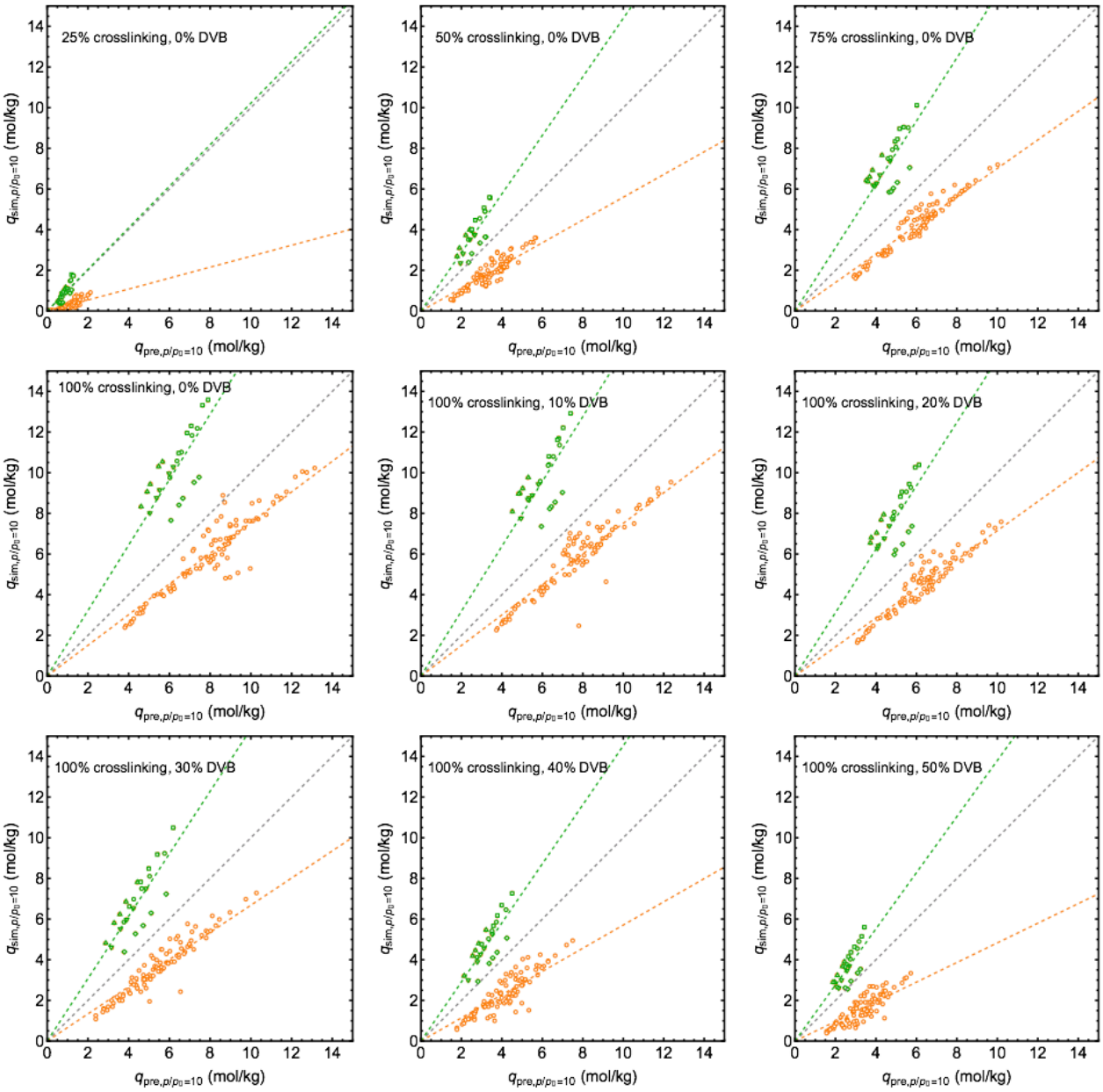

Figure S7: Comparison between $q_{sim,P/P0=10}$ and $q_{pre,P/P0=10}$ for molecule-sample pairs of each HCP. The data of group_1 (orange) and data of group_2 (green) are fitted to y=A*x respectively. For example, in HCP with 100% crosslinking and 0% DVB, we obtain fitted line y=0.79x for group_1 (orange dashed line) and y=1.69x for group_2 (green dashed line).

Table S4. List of scaling factors as function of degrees of crosslinking and percentages of DVB of HCPs, for molecules having critical temperature larger (group 1) or slightly smaller (group 2) than 300 K.

***x*=Crosslinking**	***y*=DVB**	**Scaling factor *s* in group 1 *s*=0.0072*x*-0.0069*y*+0.084**	**Scaling factor *s* in group 2 *s*=0.0087*x*-0.0066*y*+0.85**
25	0	0.264	1.07
50	0	0.444	1.29
75	0	0.624	1.50
100	0	0.804	1.72
100	10	0.735	1.65
100	20	0.666	1.59
100	30	0.597	1.52
100	40	0.528	1.46
100	50	0.459	1.39

5) Estimated selectivity of molecular pairs using Freeman's model

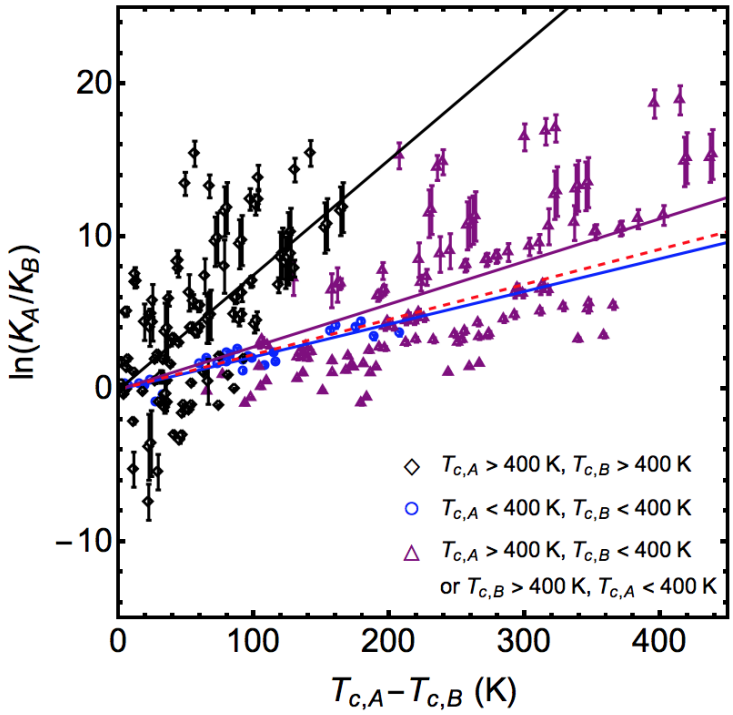

Figure S8: The median of log of Henry's constant ratio for each molecular pair as function of the critical temperature difference. The error bars represent the standard deviation of data among realizations of HCPs. There are 3 fitted lines obtained by fitting the data to Freeman's model, giving fitted factor N=0.075 K^{-1} and R^2=2.859 (R^2 is the mean absolute standardized residuals) when $T_{c,A}$ and $T_{c,B}$ are larger than 400 K (black), N=0.021 K^{-1} and R^2=0.448 when $T_{c,A}$ and $T_{c,B}$ are smaller than 400 K (blue), and N=0.028 K^{-1} and R^2=2.933 when $T_{c,A}$ and $T_{c,B}$ are larger than and smaller than 400 K respectively (purple). The red dashed line shows the prediction of log of Henry's constant ratio using N=0.023 K^{-1} of Freeman's model.

We find that Henry's constant and critical temperature of most of molecular pairs considered in this study do not obey a linear relationship, and they deviate far from the relationship with factor N=0.023 K^{-1} of Freeman's model (red dashed line in Figure S8). For the data where the critical temperatures of the two molecules in those pairs are both greater than 400 K, the fitted N equals to 0.075 K^{-1}. And for pairs in which the critical temperature of one of the molecules is larger than 400 K, and that of the other molecule is not, the data gives N of 0.028 K^{-1}. Only for the data having critical temperatures of two molecules less than 400 K, a strong linear correlation of Henry's constant and critical temperature, is obtained N equal to 0.021 K^{-1}, i.e. similar to the factor N in Freeman's model. Previous works of Freeman's investigated the relationship between solubility and critical temperature, or the relationship between binding energy and critical temperature, for molecules with critical temperature less than 400 K.[10-12] That might explain why Freeman's model works well only for data in the limited temperature domain.

6) Examples: check the convergence of GCMC simulations

In order to check the convergence of the adsorption loadings if 10^5 Monte Carlo (MC) cycles are used for equilibrium and production runs respectively, we did following tests (Table S5), considering the adsorption for 2 kind of molecules with different sizes in 2 HCPs having various pore volumes, and different number of MC cycles. The low and high pressures tested are according to the vapor pressure of each molecule.

The rolling average of adsorption loadings as function of MC cycles of tests are shown in Figure S9 and Figure S10. By comparing the adsorption loadings listed in Table S5, we know that the adsorption loadings from GCMC simulations using RASPA get converged if 10^5 MC cycles for equilibrium run and 10^5 MC cycles for production run are used.

Table S5.

HCP	**Molecule**	**Number of MC cycles for equilibrium and production respectively**	**(300 K) Pressure (Pa)**	**Adsorption loading (mol/kg)**
Sample 1 of HCP 100% crosslinking 0% DVB	$C_8H_{18}O$	10^5	0.004664	0.53343
		10^6		0.53688
	CH_4	10^5	45200.0	0.28904
		10^6		0.28927
		10^5	45200000.0	9.74253
		10^6		9.73844
Sample 1 of HCP 100% crosslinking 50% DVB	$C_8H_{18}O$	10^5	0.004664	0.02853
		10^6		0.02938
		10^5	466.4	0.80764
		10^6		0.77447
	CH_4	10^5	45200.0	0.15866
		10^6		0.15846
		10^5	45200000.0	4.52557
		10^6		4.52478

(a) (b)

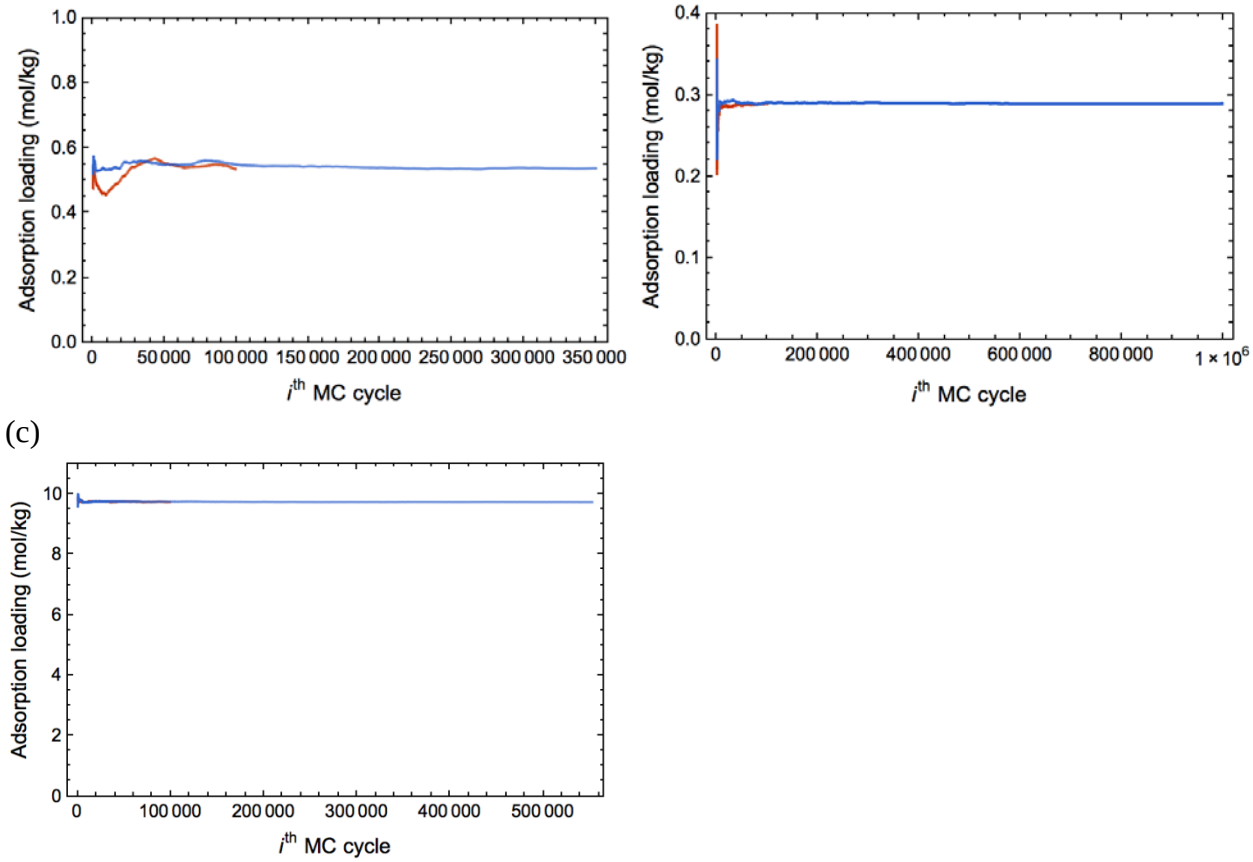

Figure S9: Rolling average of adsorption loading as function of MC cycle, where red line shows the data when 10^5 MC cycles are used for equilibrium and production runs respectively, and blue line shows the data when 10^6 MC cycles are used for equilibrium and production runs respectively. (a) $C_8H_{18}O$ in sample 1 of HCP with 100% crosslinking and 0% DVB at 300 K and 0.004664 Pa. CH_4 in sample 1 of HCP with 100% crosslinking and 0% DVB (b) at 300 K and 45200 Pa, and (c) at 300 K and 45200000 Pa.

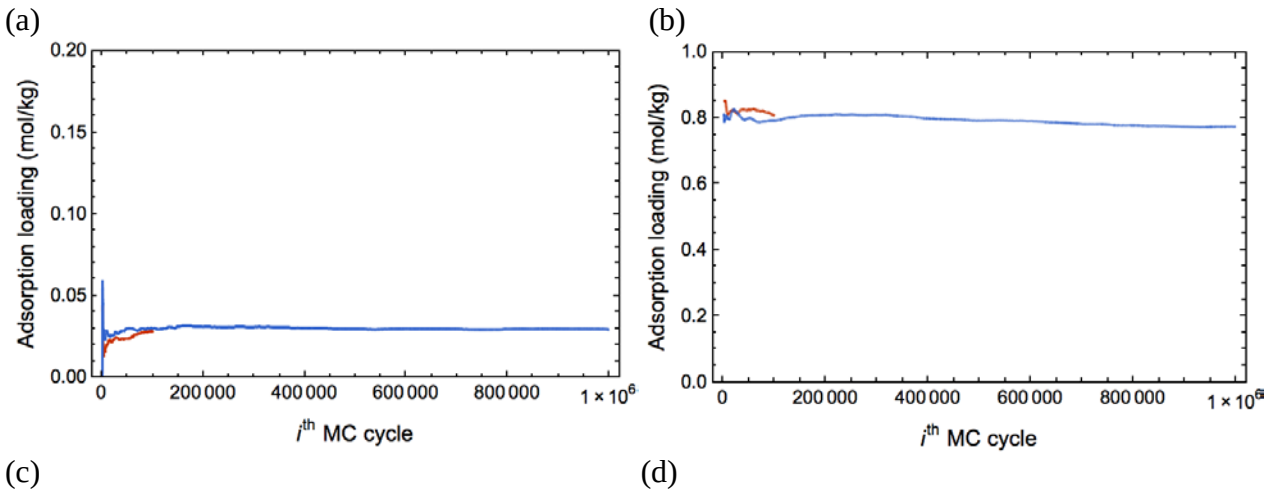

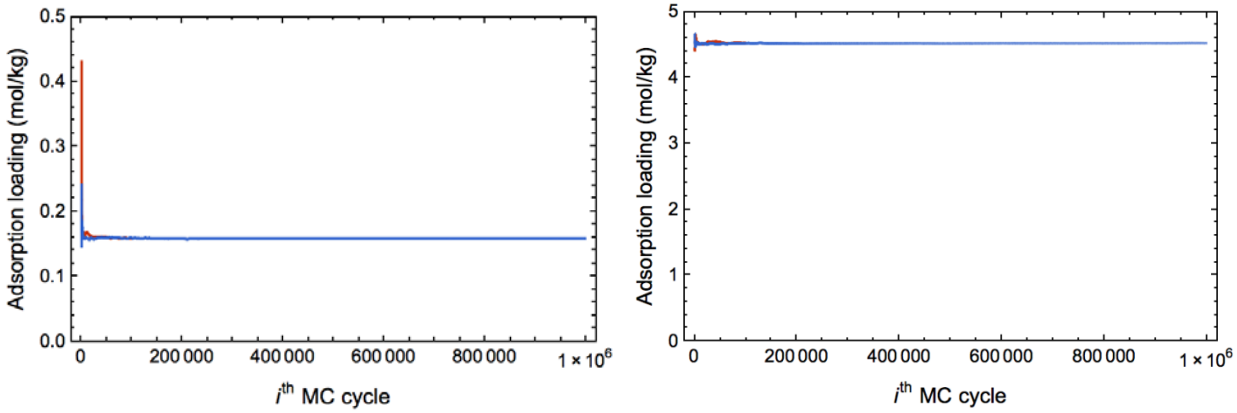

Figure S10: Rolling average of adsorption loading as function of MC cycle, where red line shows the data when 10^5 MC cycles are used for equilibrium and production runs respectively, and blue line shows the data when 10^6 MC cycles are used for equilibrium and production runs respectively. $C_8H_{18}O$ in sample 1 of HCP with 100% crosslinking and 50% DVB (a) at 300 K and 0.004664 Pa, and (b) at 300 K and 466.4 Pa. CH_4 in sample 1 of HCP with 100% crosslinking and 50% DVB (c) at 300 K and 45200 Pa, and (d) at 300 K and 45200000 Pa.

7) Data shown in all figures in the main manuscript

Data for all figures in the form of Excel spreadsheets are available in a separate .zip file with the file names noted below.

Figure 1a: XYZ files of 4 monomers: Fig1_DVB.xyz, Fig1_mVBC.xyz, Fig1_pVBC.xyz and Fig1_STR.xyz
Figure 1b: CIF file for sample 1 of HCP with 100% crosslinking and 10% DVB: PolymerModels(cif)/100crosslink_10DVB_1.cif

Figure 2a and 2b: hcps_properties.xlsx

Figure 3a: simulation/CH4_methane_sim.xlsx
Figure 3b: simulation/C8H18O_octan-1-ol_sim.xlsx

Figure 4: HenryConstant.xlsx

Figure 5a: Fig5a_QsimQpre_group1.xlsx and Fig5a_QsimQpre_group2.xlsx
Figure 5b: Fig5b_QsimQpre_group1.xlsx and Fig5b_QsimQpre_group2.xlsx
Figure 5c and 5d: Table S4 in SI

Figure 6: RelativeError.xlsx

Figure 7a and 7b: Selectivity.xlsx

8) Supporting Information References

(1) *NIST Chemistry WebBook*; Linstrom, P. J.; Mallard, W. G., Eds.; NIST Standard Reference Database Number 69; National Institute of Standards and Technology: Gaithersburg MD, http://webbook.nist.gov, (retrieved Novermber 30, 2017).

(2) Wick, C. D.; Martin, M. G.; Siepmann, J. I. Transferable Potentials for Phase Equilibria. 4. United-Atom Description of Linear and Branched Alkenes and Alkylbenzenes. *J. Phys. Chem. B* **2000,** *104*, 8008-8016.

(3) Chen, B.; Potoff, J. J.; Siepmann, J. I. Monte Carlo Calculations for Alcohols and Their Mixtures with Alkanes. Transferable Potentials for Phase Equilibria. 5. United-Atom Description of Primary, Secondary, and Tertiary Alcohols. *J. Phys. Chem. B* **2001,** *105*, 3093-3104.

(4) Stubbs, J. M.; Potoff, J. J.; Siepmann, J. I. Transferable Potentials for Phase Equilibria. 6. United-Atom Description for Ethers, Glycols, Ketones, and Aldehydes. *J. Phys. Chem. B* **2004,** *108*, 17596-17605.

(5) Wick, C. D.; Stubbs, J. M.; Rai, N.; Siepmann, J. I. Transferable Potentials for Phase Equilibria. 7. Primary, Secondary, and Tertiary Amines, Nitroalkanes and Nitrobenzene, Nitriles, Amides, Pyridine, and Pyrimidine. *J. Phys. Chem. B* **2005,** *109*, 18974-18982.

(6) Lubna, N.; Kamath, G.; Potoff, J. J.; Raj, N.; Siepmann, J. I. Transferable Potentials for Phase Equilibria. 8. United-atom Description for Thiols, Sulfides, Disulfides, and Thiophene. *J. Phys. Chem. B* **2005,** *109*, 24100-24107.

(7) Cortes Morales, A. D.; Economou, I. G.; Peters, C. J.; Siepmann, J. I. Influence of Simulation Protocols on the Efficiency of Gibbs Ensemble Monte Carlo Simulations. *Mol. Simul.* **2013,** *39*, 1135-1142.

(8) Dinpajooh, M.; Bai, P.; Allan, D. A.; Siepmann, J. I. Accurate and Precise Determination of Critical Properties from Gibbs Ensemble Monte Carlo Simulations. *J. Chem. Phys.* **2015,** *143*, 114113.

(9) Martin, M. G.; Siepmann, J. I. Transferable Potentials for Phase Equilibria. 1. United-Atom Description of n-Alkanes. *J. Phys. Chem. B* **1998,** *102*, 2569-2577.

(10) Freeman, B. D. Basis of Permeability/Selectivity Tradeoff Relations in Polymeric Gas Separation Membranes. *Macromolecules* **1999,** *32*, 375-380.

(11) Robeson, L. M.; Freeman, B. D.; Paul, D. R.; Rowe, B. W. An Empirical Correlation of Gas Permeability and Permselectivity in Polymers and its Theoretical Basis. *J. Membr. Sci.* **2009,** *341*, 178-185.

(12) van der Vegt, N. F. A.; Kusuma, V. A.; Freeman, B. D. Basis of Solubility versus T_C Correlations in Polymeric Gas Separation Membranes. *Macromolecules* **2010,** *43*, 1473-1479.